Abnormal Golgi morphology and decreased COPI function in cells with low levels of SMN

Custer SK[1], Foster JN, Astroski JW, Androphy EJ

Sara K Custer, PhD (corresponding author)
skcuster@iu.edu
Walther Hall, R3 C636
980 West Walnut Street
Indianapolis, IN 46202
317-278-7319

Joycelynn N Foster, MS
joyfoste@umail.iu.edu

Jacob W Astroski, BS
jastrosk@umail.iu.edu

Elliot J Androphy, MD
eandro@iu.edu

Keywords:
Spinal Muscular Atrophy
COPI
Golgi
coatomer
motor neuron disease
survival motor neuron

Abstract

We report here the finding of abnormal Golgi apparatus morphology in motor neuron like cells depleted of SMN as well as Golgi apparatus morphology in SMA patient fibroblasts. Rescue experiments demonstrate that this abnormality is dependent on SMN, but can also be rescued by expression of the COPI coatomer subunit alpha-COP. A motor neuron-like cell line containing an inducible alpha-COP shRNA was created to generate a parallel system to study knockdown of SMN or alpha-COP. Multiple assays of COPI-dependent intracellular trafficking in cells depleted of SMN demonstrate that alpha-COP function is suboptimal, including failed sequestration of plasma membrane proteins, altered binding of mRNA, and defective targeting and transport of Golgi-resident proteins.

1. Introduction

Spinal Muscular Atrophy (SMA) is a progressive neurodegenerative disease characterized by loss of alpha motor neurons. Understanding the basic cellular processes that underlie this neuronal loss opens up potential avenues for novel therapeutic interventions in SMA as well as other motor neuron diseases. We have focused our recent studies on the interaction between SMN and the alpha subunit of the COPI coatomer. As we previously reported, the alpha-COP and SMN proteins interact and co-migrate in axons of cultured neurons (Peter et al., 2011). In cells depleted of alpha-COP, there was decreased delivery of SMN protein to the leading edge of the cell. We also showed that in motor neuron-like cells, depletion of SMN resulted in poor neurite outgrowth, which could be rescued by expressing SMN but not SMN mutants that do not bind to alpha-COP (Custer et al., 2013). Interestingly, heterologous expression of alpha-COP in these SMN depleted cells produced a robust rescue of neurite outgrowth comparable to that generated by expression of human SMN. NSC-34 cells expressing shRNA against murine alpha-COP were unable to produce neurites. This phenotype could be rescued by expression of wild type alpha-COP but not by a point mutant of alpha-COP that no longer bound SMN (Li et al., 2015). These studies demonstrate the biological relevance of the interaction between SMN and alpha-COP.

For the research discussed here, we sought to assess the function of the COPI coatomer in cells depleted of SMN. In mammals, coatomer function appears to be important for maintenance of neuronal health. The *mdf* mutant mouse develops muscle wasting, motor neuron loss and cerebellar degeneration as a result of mutations in Scyl1, a protein that binds to the COPI coat complex and regulates Golgi-ER retrograde trafficking (Schmidt et al., 2007). Mice lacking Scyl1 develop a motor neuron disease similar to amyotrophic lateral sclerosis (ALS) (Pelletier et al., 2012). Mice with a mutation in delta-COP/archain 1 develop Purkinje neuron degeneration and cerebellar atrophy (Xu et al., 2010). A family with autosomal dominant mutations in alpha-COP developed exercise-induce dyskinesia along with a constellation of autoimmune issues (Watkin et al., 2015). These findings underscore the importance of COPI function in maintaining neuronal health, especially in large neurons with heavy transport burdens such as Purkinje cells and alpha motor neurons. The majority of COPI is resident at the Golgi apparatus, and it regulates intracellular trafficking between the endoplasmic reticulum (ER) and the Golgi (Szul and Sztul, 2011). COPI coatomer function is particularly important for maintenance of normal Golgi morphology both in resting cells and in cells entering mitosis. In HeLa cells, abnormal Golgi morphology was observed after depletion of alpha, beta or beta'-COP (Razi et al., 2009). Abnormal Golgi morphology has been observed in numerous models of motor neuron diseases including ALS caused by mutations in superoxide dismutase 1 (SOD1) (van Dis et al., 2014), TDP-43, FUS and optineurin (OPTN) (Fifita et al., 2017; Soo et al., 2015). It has also been reported in various mouse models of

motor neuron disease including the pmn mouse (progressive motor neuropathy) (Bellouze et al., 2014). Golgi fragmentation has been described in postmortem studies of Alzheimer's (Ayala and Colanzi, 2017) and Parkinson's disease brains (Fujita et al., 2006).

Here we report finding of abnormal Golgi morphology in both SMN depleted NSC-34 cells and fibroblasts from Type I and Type II SMA patients, indicating that perhaps the COPI coatomer function is impaired under conditions of SMN depletion. To assay the impact of impaired COPI function on neuronal cells, we studied two doxycycline inducible shRNA cell lines, our previously published alpha-COP knockdown SH-SY5Y cell line (1-15d) (Peter et al., 2011) and a newly generated line in NSC-34 cells using the same alpha-COP shRNA. These cells were derived from the same parental NSC-34 line as our inducible shRNA knockdown of SMN for a direct comparison of SMN depletion and alpha-COP depletion.

We demonstrate Golgi abnormalities in both NSC-34 cells and SMA patient fibroblasts can be rescued by over-expression of SMN and that its interaction with alpha-COP was required for this rescue. Expression of alpha-COP also restored normal Golgi morphology in these cultures but this rescue was not dependent on the ability to bind SMN. We assayed a number of intracellular trafficking pathways controlled by COPI coatomer in both alpha-COP and SMN depleted cells to determine if the COPI coatomer function was intact under conditions of low SMN. We find that there is a mild defect in COPI-dependent trafficking of the Kainate receptor subunit (KA2) to the plasma membrane in SMN depleted cells, which was not detected in cells expressing mutant SOD1. SMN depleted cells are also unable to properly localize the COPI target KDEL receptor. Finally, despite their abnormal Golgi morphology, SMN depleted cells did not exhibit increased ER stress as evidenced by their lack of sensitivity to thapsigargin. We conclude that although COPI-dependent intracellular trafficking appears dysregulated after SMN knockdown, the ER-Golgi system is not sufficiently altered to induce ER stress.

2. Results

2.1 Alpha-COP is required for SMN localization to the growth cone of NSC-34 cells

We had previously demonstrated that depletion of alpha-COP in SH-SY5Y cells resulted in a failure of SMN protein to traffic to the leading edge of filipodia (Peter et al., 2011). We found a similar result in the motor neuron-like NSC-34 cells. NSC-34 cells were grown in differentiation conditions for 48 hours to induce neurite outgrowth followed by infection with lentiviral particles expressing shRNA against murine alpha-COP or control shRNA against green fluorescent protein (GFP). Western blotting of whole cell lysates confirmed that alpha-COP protein levels were reduced to 41 +/- 4% of control cultures, while levels of SMN protein were unchanged (Fig 1a). After 48 hours of alpha-COP knockdown, immunofluorescence microscopy revealed there was a reduction in the amount of SMN protein at the growth cone despite no change in overall levels of SMN protein, indicating that alpha-COP is involved in the delivery of SMN to the tips of growing processes (Figure 1b). 15-20 growth cones per condition were analyzed from three separate knockdown and control cultures, and decreased SMN fluorescence intensity was observed in 81% of cells after alpha-COP knockdown.

2.2 Abnormal Golgi morphology and SMN depletion in NSC-34 cells

Golgi fragmentation has been reported in models of SOD1-induced ALS, which was accompanied by reduction in the levels of β-COP protein (Bellouze et al., 2016). To begin investigations of the outcome of low SMN protein on the Golgi, we used doxycycline-induced SMN reduction NSC-34 clone 4-56 cells. Western blotting of total cell lysates demonstrated that

SMN knockdown did not decrease levels of alpha-COP (Figure 1c). Immunofluorescent staining for the cis-Golgi marker GM130 revealed a significant fraction of cells with dispersal of the Golgi into a diffuse punctate pattern along with a similar redistribution of the alpha-COP localization after SMN depletion, (Fig 1d, $p<0.05$ by Chi^2). ImageJ was used to quantify the number of co-localized pixels between alpha-COP and GM130 before and after SMN knockdown, demonstrating a significant decrease in overlap as assessed by Mander's co-efficient of colocalization ($p<0.05$ by Student's t-test). (Figure 1f, 1e). There was also significant difference in the overlap between GM130 and alpha-COP staining as assessed by Pearson's co-efficient of colocalization ($P<0.01$ by Student's t-test) These findings indicate that alpha-COP function at the Golgi may be impaired under conditions of low SMN protein.

2.3 Alpha-COP depletion phenocopies SMN depletion in NSC-34 cells

One of the phenotypes most often described in cells depleted of COPI coatomer components and its binding partners is altered morphology of the Golgi apparatus (Bellouze et al., 2016; Razi et al., 2009). It has been reported that after acute depletion of SMN, cells showed poor re-polymerization of the microtubule network following treatment with nocodazole, which was attributed to increased expression of Stathmin (Wen et al., 2010). A similar finding has been reported after knockdown of COPI components where it was demonstrated that COPI function is required for Golgi reassembly after nocodazole treatment (Hehnly et al., 2010). We used the doxycycline-induced alpha-COP shRNA in SH-SY5Y cells (clone 1-15d) to examine the impact of decreased COPI function on Golgi morphology. As we have previously published, doxycycline treatment results in consistent depletion of alpha-COP protein, followed by a reduction in epsilon-COP (Custer and Androphy, 2014). Alpha-COP and epsilon-COP are tightly bound the in the COPI B-subcomplex and depend on each other for stability (Gu et al., 1997; Lee and Goldberg, 2010). In these 1-15d cells, knockdown of alpha-COP for 48 hours resulted in extremely compact GM130 staining in over 90% of cells as scored by a blinded observer. Measurement of Golgi size in five random visual fields showed a decrease in GM130-positive area of 60% +/- 7%. This is in contrast to the diffuse GM130 staining pattern that was reported in HeLa cells after knockdown of alpha/beta or beta'-COP (Razi et al., 2009) (Figure 2a, b). Quantification of GM130-positive area from three randomly chosen visual fields showed a decrease of 60% after depletion of alpha-COP. Treatment with nocodazole leads to a punctate GM130 staining pattern, and complete loss of Golgi integrity due to loss of the microtubule network (Thyberg and Moskalewski, 1985). After nocodazole washout, GM130 staining returned to its normal juxtanuclear pattern in control cells. However, in alpha-COP depleted cells, Golgi reformation was significantly delayed (Figure 2c, d). This experiment demonstrates that proper recovery from nocodazole depends on COPI function, and could explain the findings that were previously attributed to increased levels of Stathmin in SMN depleted cells (Wen et al., 2010).

To provide a parallel system in which to study COPI coatomer function in motor neuron-like cells, we made use of the parental NSC-34 line, clone #4, which expresses the reverse tet-transactivator. These cells were transfected with the same shRNA plasmid used to generate our previously published SH-SY5Y model of alpha-COP knockdown (shRNA 1-15). Multiple clonal lines were isolated and we selected a clone that demonstrated robust doxycycline-induced alpha-COP depletion after 48 hours, hereafter referred to as NSC-34 clone 4-1-15. This allowed us to perform all further experiments examining SMN or alpha-COP depletion in identical cell culture systems. Comparison of Golgi morphology in the SMN or alpha-COP knockdown NSC-34 cells by immunofluorescence shows similar phenotypes of diffuse, punctate GM130 staining (Figure 2e). This diffuse GM130 staining was not observed in control NSC-34 cells expressing shRNA against luciferase (not shown) indicating that this is not simply a

response of NSC-34 cells to doxycycline. Figure 2f shows representative Western blots from line 4-56 and line 4-1-15 and confirms that levels of SMN were not affected by knockdown of alpha-COP (1.008 +/- 0.05 after DOX treatment compared to control cells when quantified from repeated experiments by densitometry). This is consistent with a previous report in NSC-34 following siRNA depletion of alpha-COP (Ting et al., 2012), and levels of alpha-COP remained steady after knockdown of SMN (0.98 +/- 0.09 after DOX treatment compared to control cells when quantified from repeated experiments by densitometry).

2.4 Golgi morphology is abnormal in SMA fibroblasts

To determine if our findings of abnormal Golgi morphology were present in other cell types, we turned to primary fibroblasts isolated from either Type I or Type II SMA patients compared to a control line isolated from a carrier parent. When scored by a blinded observer, we found a similar phenotype of dispersed punctate GM130 staining in the SMA cells compared to the control line (Figure 3a). Figure 3b shows examples of normal, intermediate and diffuse Golgi morphology as visualized by GM130 immunofluorescence (GM130 in green, tubulin in red, and DAPI in blue). These images were used to guide a blinded observer in scoring the Golgi morphology in each of the four patient fibroblast populations. Scoring of Golgi morphology revealed a statistically significant increase in the number of cells with diffuse GM130 staining (Figure 3c, $p<0.001$ by Chi^2 compared to controls). Previous reports have described fragmentation of the Golgi in NSC-34 cells transfected with FUS harboring ALS-associated mutations (Farg et al., 2013). We did not find significant alterations in Golgi morphology in cultured fibroblasts from a patient with ALS caused by mutation in FUS (cell line ND29563), This line carries a synonymous R522R mutation, and has been reported in controls (Corrado et al., 2010; Tarlarini et al., 2015) compared to the R521 mutations characterized by Farg and colleagues.

2.5 Rescue of Golgi morphology by SMN does not depend on alpha-COP binding

To determine whether the Golgi abnormalities were SMN dependent, we infected SMA fibroblast cultures with lentiviral particles expressing FLAG-tagged human SMN (Wang et al., 2013). Expression of wild type SMN produced a statistically significant shift of Golgi morphology back towards normal. We have previously described the di-lysine domain in SMN exon 2b, which mediates alpha-COP. Mutation of either the lysines at position 76/77 or 82/83 eliminated the ability of GST-tagged exon 2b to immune-precipitate alpha-COP protein (Custer et al., 2013). To determine if alpha-COP binding was required for SMN to rescue Golgi morphology in the patient fibroblast culture system, we used site-directed mutagenesis to convert both dilysine domains to alanine (Figure 4a). This construct is referred to as SMN-ΔΔ. Immunoprecipitation from patient fibroblasts infected with either wild type-SMN or SMN-ΔΔ confirmed that only wild type SMN was able to co-immunoprecipitate alpha-COP (Figure 4b). Immunofluorescent staining revealed a diffuse distribution of the FLAG-SMN (Figure 4c). GM130 morphology was again assessed in a blinded protocol, and quantitation shows that both wild type and SMN-ΔΔ were able to restore the Golgi morphology of SMA patient fibroblasts to normal. Chi-squared comparison of the distribution of Golgi morphology between 3813 alone or 3813 with SMN-wt showed that the rescue was significant ($p<0.01$) and analysis of 3813 with SMN-ΔΔ yielded similar results ($p=0.002$). There was no statistically significant difference between 3813 cells treated with SMN-wt and SMN-ΔΔ ($p=0.12$).

Previously, we showed that the ability of alpha-COP and SMN to support neurite outgrowth required reciprocal interactions – SMN that did not bind alpha-COP was unable to increase

neurite length and similarly, alpha-COP that did not bind SMN was unable to restore neurite outgrowth in NSC-34 cells after knockdown of endogenous alpha-COP. To determine if reciprocal interaction is required for Golgi morphology in SMA patient fibroblasts, we infected the cells with lentivirus expressing either FLAG-tagged wild type alpha-COP or alpha-COP carrying the Y1090H mutation, which is defective for binding to SMN and is unable to rescue neurite length in alpha-COP depleted NSC-34 cells (Li et al., 2015). Immunofluorescent microscopy with the FLAG antibody demonstrated accumulation of alpha-COP at the Golgi apparatus in infected cells (Figure 4d). In agreement with the findings in cells rescued with SMN, both wild type and Y1090H alpha-COP were able to restore normal Golgi morphology in SMA patient fibroblasts; however, treatment with Y1090H did not reach statistical significance ($p=0.061$ compared to 3813 alone by Chi-squared analysis.) Taken together, these data indicate that the action of alpha-COP in this context is independent of SMN association (Figure 4f.)

2.6 Alpha-COP dependent intracellular trafficking is affected under conditions of low SMN

In addition to facilitating Golgi-ER transport, the COPI complex can retain proteins in the ER, as is the case for the kainite receptor subunit KA2. In the absence of other receptor subunits, KA2 is sequestered in the ER via interaction between a dibasic motif in its cytoplasmic tail and COPI (Ren et al., 2003). Depletion of COPI components prevents this interaction and allows monomeric KA2 to reach the membrane (Vivithanaporn et al., 2006). We used a myc-tagged KA2 construct transfected into NSC-34 cells to monitor COPI-dependent trafficking. The myc-tagged KA2 was readily detected in whole cell NSC-34 cells lysates after transient transfection (Figure 5a). RT-PCR analysis of NSC-34 cells under differentiation conditions showed expression of GluR6, which is required for function KA2 heterodimers and transport to the plasma membrane (not shown). As a positive control, we transfected the myc-KA2 into 4-1-15 NSC-34 cells where the alpha-COP had been depleted by doxycycline treatment for 48 hours. Using a cell impermeant biotin, extracellular proteins were labeled and then precipitated using streptavidin beads. As expected, given previously published results from cells deficient in epsilon-COP, there was a 2.4 fold (SEM 0.31) increase in myc-KA2 presence at the plasma membrane after alpha-COP knockdown (Figure 5a). The experiment was then performed in NSC 4-56 cells following 48 hours of SMN knockdown. Although the increase was smaller than with alpha-COP knockdown, there was an approximately 1.4 fold increase (SEM 0.21) in the levels of myc-KA2 at the plasma membrane after SMN knockdown (Figure 5a, quantified in 5b from 3 independent experiments). Reports in cell culture and animal models of SMA have indicated that there may be defects in recycling of certain cargoes at the plasma membrane (Dimitriadi et al., 2016; Riessland et al., 2017). To insure that the increase in KA2 was not simply a reflection of poor plasma membrane recycling, we measured the levels of EGF receptor (EGFR) in the NSC-34 cells after SMN depletion. In this case, there was no change in EGFR levels at the plasma membrane after SMN depletion, indicating that the increase in plasma membrane KA2 was a read out of COPI coatomer function rather than ineffective membrane recycling in general (Figure 5a). As a second control, we measured endocytosis of the plasma membrane myc-KA2 in NSC-34 4-56 cells by exposing them to cell impermeant biotin followed by a return to the tissue culture incubator for 30 minutes. Any remaining cell surface biotinlyation was stripped, and the amount of internalized myc-KA2 was compared to the levels present at the plasma membrane to determine the fraction that became intracellular. Figure 5c shows a representative western blot demonstrating similar amounts of biotinylated myc-KA2 were endocytosed during the 30-minute incubation. For loading control, blots were probed with streptavidin-HRP, and knockdown of SMN was confirmed in the total lysate. 5d shows the quantification of three separate experiments quantified by imageJ and compared by Student's t-test, which revealed that there was no significant decrease in the amount of myc-

KA2 that was endocytosed following depletion of SMN. This further supports the conclusion that for this protein, the increase at the plasma membrane is due to poor COPI function rather than SMN-dependent changes in global rates of endocytosis. To assess COPI function in an independent model of motor neuron disease; we examined NSC-34 cells expressing doxycycline inducible SOD1 protein, either wild type or the G93A mutant that is associated with familial ALS (Mali and Zisapel, 2010). These cells did not exhibit an increase in myc-KA2 at the cell surface after SOD1 induction (Figure 5e). We have previously reported that alpha-COP binds a number of mRNAs, and we predict that these COPI associated mRNA are transported in COPI coated vesicles (Todd et al., 2013). Analysis of the RNA-seq results of mRNA immunoprecipitated with alpha-COP under control conditions or after SMN knockdown predicted that a small subset of the alpha-COP associated mRNA were SMN dependent. We used quantitative RT-PCR on mRNA that co-precipitated with alpha-COP after formaldehyde cross-linking using NSC-34 4-56 cells before and after SMN knockdown and found that Irgm2 mRNA association with alpha-COP was decreased approximately 7 fold following depletion of SMN. As a positive control, we confirmed that the amount of Irgm2 pulled down after knockdown of alpha-COP was also significantly reduced (Figure 5f, $p<0.05$ by Student's t-test). The total levels of Irgm2 transcript were not affected by loss of either SMN or alpha-COP. Irgm2 protein is localized exclusively to the Golgi (Zhao et al., 2010) and so perhaps its mRNA is less likely to associate with alpha-COP when the Golgi apparatus is dissociated under conditions of low SMN.

2.7 SMN knockdown alters localization of proteins that shuttle between the Golgi and the ER

As another measure of COPI-dependent intracellular trafficking, we used a temperature sensitive mutant of vesicular stomatitis virus G protein (VSVGts045) fused to the KDEL receptor (KDELR) and Yellow Fluorescent Protein (YFP) to assess retrograde trafficking from the Golgi to the ER. Unlike membrane-bound ER residents that use direct COPI binding to concentrate in COPI vesicles, soluble ER-resident proteins use C-terminal KDEL sequences to bind the KDELR, which mediates their COPI-dependent retrieval to the ER (Raykhel et al., 2007; Spang and Schekman, 1998). The YFP-VSVGts045-KDELR chimera cycles between the ER and the cis-Golgi at the permissive temperatures; however, at the restrictive temperatures, protein that has undergone retrograde trafficking becomes trapped in the ER due to misfolding, providing a measure to examine COPI-dependent retrograde traffic (Yang et al., 2008). We have previously used this system to characterize the ability of alpha-COP mutants that do not bind SMN to support normal COPI vesicle transport (Li et al., 2015). This assay was performed in both SH-SY5Y and NSC-34 cells following doxycycline-inducible alpha-COP knockdown. Control cells trafficked in YFP-KDELR-VSVG protein normally, with mostly Golgi-like YFP signal under permissive temperatures and shifting to a reticular ER pattern of fluorescence when moved to the restrictive temperature. Following alpha-COP knockdown, an increased number of cells retained the YFP fluorescence in a Golgi pattern, indicating a failure of COPI-dependent Golgi-ER transport (Figure 6a). When transfected into control NSC-34 cells, the YFP-KDELR-VSVG plasmid successfully localized to the Golgi under permissive temperatures and redistributed to the ER at the restrictive temperature. However, after SMN knockdown, the YFP-KDELR-VSVG failed to properly localize to the Golgi at permissive temperatures, but was found in a diffuse reticular pattern, indicating that intracellular protein localization signals were disrupted in these cells and a protein destined for the Golgi was improperly retained in the ER (Figure 6b). In attempt to overcome the abnormal trafficking of the YFP-KDELR-VSVG reporter in SMN depleted NSC-34 cells, we repeated these experiments in HeLa cells, in which this reporter has been extensively used (Burman et al., 2008; Luna et al., 2002). HeLa cells were transfected with either a scramble shRNA, or an shRNA against human SMN, which reduces levels of SMN

to approximately 25% of normal (Han et al., 2016). Control cells trafficked the reporter as expected, with YFP fluorescence showing a Golgi-type pattern at the permissive temperature and an ER-type pattern when shifted to the restrictive temperature for 1 hour. Cells that were transfected with both the reporter and the shRNA against SMN showed a Golgi-like pattern of YFP fluorescence at the permissive temperature, After a 1 hour shift to the restrictive temperature, 42% of cells showed a shift to an ER-like pattern compared to control cells (Figure 6C). However, after 2hrs, there was no statistically significant difference between control cells and SMN knockdown cells with regard to ER localization, showing that retrograde Golgi to ER trafficking in SMN depleted cells is occurring, but at a much slower rate than in controls.

2.8 SMN knockdown does not increase sensitivity to thapsigargin

As a final assessment of Golgi/ER function in the SMN depleted cells, we compared the response of NSC-34 cells to thapsigargin after knockdown of alpha-COP or SMN. Reports have indicated that there are signs of ER stress in models of SMA (Ng et al., 2015). In models of COPI dysfunction, poor retrieval of escaped ER resident proteins as well as accumulation of autolysosomes puts stress on the ER and can induce the unfolded protein response (Izumi et al., 2016). If the dissociated Golgi apparatus seen in the SMA cells were not functioning correctly, we would expect this to result in increased stress on the ER. To test this hypothesis, we exposed cells to the ER toxin thapsigargin. If the ER were stressed, there should be an increased sensitivity to thapsigargin. Knockdown of alpha-COP for 48 hours in NSC-34 4-1-15 cells resulted in a significant leftward shift in the dose response cell death curve (p=0.021 by ANOVA). However, after 48 hours of SMN knockdown, NSC-34 cells did not display significantly increased sensitivity to thapsigargin (Figure 7). This experiment indicates that COPI-dependent trafficking between the Golgi and the ER is not sufficiently abnormal to stress the ER to a degree that it demonstrates increased sensitivity to thapsigargin.

3. Discussion

We have shown in several model systems that expression of alpha-COP can compensate for low levels of SMN to restore normal neurite outgrowth. Here we report the finding that in both NSC-34 motor neuron-like cells and human fibroblasts derived from Type I and Type II SMA patients, under conditions of low SMN, there is an increased incidence of abnormal Golgi apparatus morphology, specifically a diffuse, punctate pattern visualized with the cis-Golgi marker GM130. This pattern has been reported as a consequence of expressing mutant proteins associated with motor neuron disease including SOD1, TDP-43 and optineurin (reviewed in (Haase and Rabouille, 2015)). Disruption of normal Golgi morphology has also been reported in cells where components of the COPI coatomer have been depleted (Razi et al., 2009). By creating a doxycycline-inducible knockdown of alpha-COP in NSC-34 cells, we were able to compare the effects of SMN and alpha-COP depletion in parallel and find that the impact on Golgi morphology is nearly identical. This finding led us to hypothesize that COPI may not function optimally under conditions of low SMN.

A primary function of the Golgi apparatus is to monitor the proper processing and sorting of proteins synthesized at the ER as they are directed to their proper locations throughout the cell. For motor neurons, optimal operation of this system may be critical to the health and maintenance of such a sizeable and dynamic cytoarchitecture. Systemic and neuron-specific knockout of the cis-Golgi structural protein, GM130, was recently reported in mice, leading to a neurodegenerative condition and demonstrating that perturbation of a cis-Golgi component results in a neurological syndrome (Liu et al., 2017). COPI function has recently been linked to two distinct human diseases. Germ line mutations in alpha-COP cause a disorder characterized by autoimmune-mediated lung disease, arthritis and exercise induced dyskinesia (Watkin et al.,

2015). Mutations in Arcn1, which encodes the delta-COP subunit, were recently identified as the cause of a cranio-facial syndrome resulting from poor transport of collagen and ER stress (Izumi et al., 2016). Additionally, numerous mouse models with mutations in COPI components develop neurological symptoms including motor neuron disease. In the Wobbler mouse model of motor neuron disease, there are reports of endosomal accumulation of the amyloid precursor protein (Palmisano et al., 2011), which is dependent of COPI function for trafficking to the trans-Golgi after recycling from the plasma membrane (Selivanova et al., 2006), indicating that COPI-dependent trafficking may be disrupted in this model of motor neuron disease as well. Together, these data indicate the COPI function is critical for proper intracellular trafficking, and that small changes can disrupt that function and lead to disease. Our findings here demonstrate subtle changes in numerous COPI coatomer functions under conditions of low SMN. This chronic disturbance in the intricate movement of proteins throughout the cell may be sufficient to induce pathological changes.

It has been demonstrated in primary cortical neuron culture that Golgi fragmentation precedes apoptosis induced by numerous insults including excitotoxicity, ER stress and reactive oxygen species. Nakagomi et al showed that interventions, which inhibited Golgi fragmentation, such as inhibition of protein kinase A, protected neuronal cells from insult (Nakagomi et al., 2008). It is possible that the Golgi fragmentation seen after SMN depletion is a response to global cellular insult, and that alpha-COP promotes survival by stabilizing the Golgi apparatus rather than restoring a specific COPI-dependent trafficking defect.

Knockdown of alpha-COP resulted in a small fraction of SMN being sequestered in the trans-Golgi network (TGN), indicating that in addition to binding SMN and co-trafficking in the axon, alpha-COP may be involved in the transport of a small amount of SMN through the secretory pathway (Ting et al., 2012). The role of this TGN-resident SMN is unclear, but addition of alpha-COP in the presence of low levels of SMN found in the pathological state may allow for proper transport of the remaining SMN protein through the secretory pathway. This may partially explain why over-expression of alpha-COP is able to compensate for loss of SMN in cell culture and animal models of SMA. The reports of Golgi abnormalities in multiple motor neuron diseases opens the possibility that alpha-COP over-expression may have therapeutic benefit beyond SMA.

4. Experimental procedures

4.1 Cell Culture

NSC-34 cells were maintained in DMEM with 10% fetal bovine serum (FBS) and Pen/Strep. SH-SY5Y cells were maintained in DMEM/F12 with 10% FBS and Pen/Strep. For transient knockdown of alpha-COP in NSC-34 cells, cultures were infected with lentivirus expressing shRNA against murine alpha-COP (TRNC0000313321) or control lentivirus expressing shRNA against GFP (Sigma SHC005). To generate the inducible alpha-COP knockdown NSC-34 cells, NSC-34 clone #4 (TetR driver alone) were transfected with pSuperior containing hairpin 1-15 against alpha-COP and selected for 14 days in 5μg/ml blasticidin and 1.5μg/ml puromycin for 10 days. After selection, single colonies were isolated. Alpha-COP knockdown was confirmed by Western blot following 48hrs of doxycycline treatment (2μg/ml) and clone 4-1-15 was used for the experiments reported here. For NSC-34 4-56, SMN knockdown was induced using 48 hours of doxycycline treatment (2 μg/ml). SMN knockdown was verified by Western blot for all experiments. SMA-derived patient fibroblasts (Coriell) were maintained in DMEM/F12 with 15% FBS and Pen/Strep. EF1a-driven FLAG-hSMN lentivirus was a generous gift from Dr. Xue-Jun

Li. The BamH1-Not1 FLAG-SMN fragment was subcloned into pCDNA3 and site-directed mutagenesis was used to mutate the dilysine motif at amino acid 76 and 82 to di-alanine. Changes were confirmed by sequencing and then the BamH1-Not1 fragment was cloned back into the EF1a lentivirus backbone. Lentivirus was generated in HEK 293-TT cells by co-transfection with PAX2 and MD2.G at a ratio of 20:15:6. The viral supernatant was collected from transfected cells after 48 hrs and concentrated by ultracentrifugation at 25,000 rpm for 90 min. The viral pellet was resuspended in PBS and aliquots were stored at 80C until use. The titer of the virus we obtained was $4x10^8$ TU/ml. SMA fibroblasts were grown on 6-well plates and transduced with $4x10^6$ lentivirus particles. FLAG-SMN expression was confirmed by Western blot analysis of whole cell lysate probed with M2 anti-FLAG antibody (1:10,000) as well as immunofluorescent microscopy. Alpha-COP shRNA lentivirus was packaged as described above and used as described previously (Li et al., 2015).

4.2 Immunofluorescence

Cells were washed in PBS and fixed for 10 minutes in 4% paraformaldehyde followed by 30 minutes blocking and permeabilization in 5% normal goat serum with 0.2% Triton-X 100. For Golgi morphology, cells were incubated over night at 4^oC with anti GM130 (BD bioscience, 1:500) and alpha-tubulin (Sigma, 1:4000). Cells were washed three times and incubated in secondary antibody (Alexa-488 and Alexa 594 1:1000) for 1 hr at room temperature. Cells were mounted in Prolong Gold with DAPI to visualize nuclei. Golgi morphology was classified as normal, intermediate, diffuse or absent by blinded observers with at least 50 cells from three separate experiments, and statistical significance was determined by Chi^2 analysis. For detection of SMN in COPA depleted NSC-34 cells, cells were plated on 18mm glass coverslips coated with PDL and cultured in DMEM/F12 with 1% FBS for 72 hours to induce neurite outgrowth. Cultures were then infected with $4x10^6$ lentivirus particles for 48 hours. Alpha-COP knockdown was confirmed by Western Blot analysis. Cells were stained with BIII-tubulin (rabbit, 1:1000 Cell Signaling Technologies) to visualize neurites and growth cones, and Mansma2 (1:50) to visualize SMN. For cells transfected with YFP-KDELR-VSVGts045 cells were immunolabeled with alpha-tubulin (Sigma, 1:5000) and Alexa 594 (goat anti-mouse 1:1000).

4.3 KA2 trafficking assay

NSC-34 cells were grown in DMEM with 10% FBS, treated with doxycycline for 24 hours to initiate shRNA knockdown of SMN or alpha-COP, followed by transfection overnight in OPTI-MEM with 2.5 μg of myc-KA2 using Lipofectamine 2000 at a ratio of 1:2.5. Following transfection, the cells were returned to DMEM/10%FBS and doxycycline was added for an additional 24 hours. Cell surface proteins were labeled using the EZlink biotinlyation kit (Thermo Fisher). To prevent effects of membrane recycling, all steps were performed at 4^oC. Biotinylated proteins were isolated using Streptavidin Dynabeads, eluted in 2X Laemmli sample buffer, and separated by SDS-PAGE. Following transfer to PVDF membrane, blots were probed with anti-myc antibody (9E10, 1:2500). Levels of myc-KA2 at the cell surface were compared to levels in total cell lysate. Densitometry was performed on at least three experiments using ImageJ. For studies of endocytosis rates, we followed the protocol described in (Gabriel et al., 2009). Briefly, NSC-34 4-56 cells were transfected with myc-KA2 followed by knockdown of SMN for 48 hours. Cells were treated with NHS-SS-Biotin, and split into two equal pellets. For plasma membrane, the pellet was washed with glycine to inhibit further biotinlyation and the pellet was lysed. For endocytosis, the pellet was resuspended in culture media and returned to the 37°C. incubator for 30 minutes. Cells were pelleted and any remaining biotin at the plasma membrane was stripped with 50mM TCEP. Endocytosis was quantified by comparing the endocytosed fraction to the plasma membrane fraction, and blotting with Streptavidin-HRP to visualize all biotinylated proteins normalized loading.

4.4 COPI-dependent Golgi-ER trafficking assay:

Assays were performed as described (Li et al., 2015). Briefly, cells were plated on glass coverslips coated with PDL and knockdown of either alpha-COP or SMN was induced by treatment with doxycycline for 48 hours followed by transfection with YFP-KDELR-VSVGts045 plasmid using Lipofectamine 2000 in OPTI-MEM overnight. Following transfection, OPTI-MEM was exchanged for DMEM with 10% FBS and doxycycline induction continued for an additional 24 hours. During this final induction of shRNA, cells were moved to the permissive temperature (32^{o}C) to accumulate YFP-KDELR-VSVGts045 in the Golgi. Cells were fixed at the indicated time points in Z-Fix to maximize YFP fluorescence. Cells were immunostained with alpha-tubulin followed by incubation with secondary antibody (Alexa 594 1:1000). For transfections in HeLa cells, SMN was knocked down by co-transfection with shRNA against human SMN (TRCN0000118702) or a scrambled control (Addgene vector #1864).

4.5 Cell Death Assays

NSC-34 cells treated with doxycycline for 48 hrs to knock down either SMN or alpha-COP, and exposed to thapsigargin overnight at concentrations from 0-10 μM (in triplicate). Cell death was assessed by AqueousOne colorimetric MTT assay using DMSO as baseline. Dose response curves from three separate experiments were combined in Graphpad PRISM. Statistical significance was determined by ANOVA with post-hoc t-test.

Acknowledgement

Thanks to Robert Kalb for SOD1-expressing NSC-34 cells, to Geoffrey Swanson for the myc-KA2 expression vector, P. Vivithanaporn for Myc-tagged KA2, Xue-Jun Li for EF1a-driven FLAG-hSMN lentivirus and Victor Hsu for the YFP-VSVGts045-KDELR reporter construct. The research reported in this publication was supported by the CureSMA Emerging Investigator Award (Custer) and by the National Institute of Neurological Disorders and Stroke under R01NS082284 and R01NS082284-S1 (Androphy). The content is solely the responsibility of the authors and does not necessarily represent the official views of the National Institutes of Health.

Figure Legends

Figure 1: Knockdown of alpha-COP alters distribution of SMN at growth cones

NSC-34 cells were differentiated in low serum media to induce neurite outgrowth, then infected with either control lentivirus expressing shRNA against GFP, or experimental lentivirus expressing shRNA against murine alpha-COP for 48 hrs. 1a) Western blotting of total cell lysates confirmed knockdown of alpha-COP without affecting levels of SMN protein. 1b) Following alpha-COP knockdown, NSC-34 cultures were fixed and immunolabeled with antibodies against SMN (Mansma2) or βIII-tubulin. Compared to control cultures, after alpha-COP knockdown, the punctate pattern of SMN immunofluorescence was absent from βIII-tubulin positive growth cones. 15-20 growth cones per condition were analyzed from three separate knockdown and control cultures, and decreased SMN fluorescence intensity was observed in 81% of cells after alpha-COP knockdown. 1c) Western blot of whole cell lysate in NSC-34 4-56 cells after 48 hrs doxycycline treatment shows robust reduction in SMN protein and no change in alpha-COP. 1d) Immunofluorescent staining of NSC-34 4-56 after 48hrs doxycycline with GM130 (red) and alpha-COP (green) shows abnormal Golgi morphology after SMN knockdown. Nuclei visualized with DAPI (blue). Quantification of Golgi morphology by a

blinded observer showed a significant shift in the distribution on normal, intermediate and diffuse GM130 staining ($p<0.05$ by Chi^2 analysis). 1e) ImageJ analysis of GM130 (red) and alpha-COP (green) co-localization before and after SMN knockdown. Co-localized pixels are displayed in white. 1f) Mander's co-efficient of co-localization from 15 cells per condition in 3 separate SMN knockdown cultures shows significantly decreased co-localization between GM130 and alpha-COP after SMN knockdown ($p<0.05$ by Student's t-test).

Figure 2: alpha-COP or SMN knockdown disrupts Golgi morphology

2a) Immunofluorescent staining of SH-SY5Y clone 1-15d shows decreased levels of alpha-COP (green) and condensed Golgi morphology (GM130, red) after treatment with doxycycline. 2b) Western blot analysis of SH-SY5Y 1-15d shows knockdown of alpha-COP and epsilon-COP after treatment with doxycycline. 2c) Alpha-COP knockdown results in decreased return to normal GM130 staining pattern following microtubule de-polymerization with nocodazole. 2d) Quantification of GM130 morphology following nocodazole washout shows decreased rate of Golgi reorganization in alpha-COP depleted SH-SY5Y 1-15d cells ($p<0.05$ by ANOVA). 2e) Immunofluorescent staining of NSC-34 clone 4-56 and 4-1-15 after doxycycline-induced knockdown of SMN and alpha-COP respectively shows dispersed GM130 staining (GM130 in green, tubulin in red, DAPI blue). 2f) Representative Western blot analysis of NSC-34 4-56 shows robust knockdown of SMN protein with doxycycline, while COPI components remain unchanged (α-COP levels were 0.98 +/- 0.09 compared to untreated). Representative Western blot analysis of two separate doxycycline-treated NSC-34 4-1-15 cultures shows knockdown of alpha-COP while levels of SMN are stable (1.008 +/- 0/05 compared to untreated).

Figure 3: Golgi morphology is abnormal in SMA patient-derived fibroblasts

3a) Immunofluorescent staining of fibroblasts for cis-Golgi marker GM130 (green) shows disrupted, diffuse Golgi morphology in Type I (9677) and Type II (3813) SMA cells compared to cells from a carrier parent (3814). Cells were labeled with α-tubulin (red) and nuclei were visualized with DAPI (blue). 3b) Examples of normal, intermediate and diffuse Golgi morphology. These examples were used by a blinded observer to score the degree of Golgi morphology abnormality in the four cell populations studied. 3c) Quantification of GM130 staining patterns by a blinded observer shows a statistically significant increase in diffuse Golgi staining in Type I and Type II SMA fibroblasts compared to the carrier parent line (Chi^2 * $p=0.0014$ ** $p<0.0001$)

Figure 4: Binding between SMN and alpha-COP is not required to restore Golgi morphology

4a) Schematic of EF1a-FLAG-hSMN lentivirus. The dilysines at position 76, 77, 82 and 83 were mutated to alanines (SMN-$\Delta\Delta$) in human SMN under control of the EF1a promoter. 4b) Cells were infected with control or $\Delta\Delta$-SMN followed by immunoprecipitation with FLAG beads. Western blot analysis of inputs shows expression of SMN constructs and endogenous alpha-COP. Immunoblotting of the FLAG-IP demonstrates that $\Delta\Delta$-SMN fails to co-immunoprecipitate endogenous alpha-COP. The reverse is seen in cells transfected with myc-alpha-COP and FLAG-SMN. Following immunoprecipitation with myc antibody, only wildtype SMN binds to myc-alpha-COP. 4c) Infection with FLAG-hSMN (red) restores normal GM130 staining (green) in SMA fibroblasts. 4d) Infection with FLAG-alpha-COP (Flag M2 immunofluorescence, green) restored GM130 staining to normal (red) compared to un-infected 3813 cells. cells. 4e) Quantification of GM130 morphology shows statistically significant rescue with both wildtype

($p<0.01$ by Chi^2) and ΔΔ-SMN ($p<0.01$ by Chi^2) in SMA fibroblasts (compared to 3813 alone). Similarly, both wildtype and Y1090H alpha-COP expression rescued GM130 morphology, although only wildtype COPA infection reached significance (3813 vs. 3813+COPAwt $p<0.01$ by $Chi^{2.}$ 3813 vs. 3813+COPA Y1090H $p=0.061$)

Figure 5: SMN depletion alters trafficking of alpha-COP cargoes

5a) Increased levels of myc-KA2 at the plasma membrane following knockdown of both alpha-COP (NSC line 4-1-15) and SMN (NSC line 4-56). Plasma membrane levels of EGFR are unchanged after SMN knockdown. 5b) Quantification of myc-KA2 levels at the plasma membrane from three separate transfections. 5c) Total, plasma membrane and endocytosed myc-KA2 in NSC-34 4-56 cells. Again, there is an increase in the level at the plasma membrane after SMN knockdown with doxycycline. To verify even loading, blots were probed with streptavidin-HRP to visualize all biotinylated proteins. 5d) Although there is a decrease in the amount of myc-KA2 that is endocytosed, quantification of three experiments shows that the decrease was not statistically significant by Student's t-test. 5e) KA2 trafficking is unaffected in NSC-34 cells expressing wildtype or ALS-associated SOD1 (G93A). 5f) Quantification of Lrgm2 transcript levels in knockdown NSC-34 cultures (SMN and alpha-COP respectively) compared to controls. Lrgm2 transcript levels are not significantly affected by loss of SMN or alpha-COP. Quantification of Lrgm2 transcript levels after formaldehyde cross-linked RNA immunoprecipitation (FL-RIP) show decreased Lrgm2 transcript pulled down with alpha-COP when SMN is depleted. As a positive control, we show that decreased amounts of Lrgm2 precipitate after knockdown of alpha-COP.

Figure 6: Golgi-ER trafficking is impaired after COPA knockdown

6a) SH-SY5Y (1-15d) and NSC-34 (4-1-15) cells lines with dox-inducible knockdown of alpha-COP were transfected with the temperature-sensitive YFP-KDELR reporter construct following knockdown of alpha-COP for 48 hours. Graphs represent the percentage of cells with Golgi-localized YFP immunofluorescence at the permissive temperature (32^oC) and after shifting to the restrictive temperature (40^o) for 1 hr. In both cell lines, knockdown of alpha-COP increases the percentage of cells that retain Golgi-localized YFP fluorescence at the restrictive temperature indicative of reduced Golgi-ER trafficking. 6b) In control NSC-34 cells, the YFP-KDELR (green) reporter traffics normally, localizing to the Golgi (GM130, red) at the permissive temperature and shifting to the ER at the restrictive temperature. Knockdown of alpha-COP in the NSC-34 cells results in retention of the YFP-KDELR (green) in the Golgi (GM130, red) at the restrictive temperature. Knockdown of SMN results in incorrect localization of the reporter even at the permissive temperature, with cells showing predominantly ER-resident YFP fluorescence rather than Golgi localization at the permissive temperature. 6c) HeLa cells were co-transfected with either a scrambled shRNA or shRNA against human SMN. At permissive temperatures, but control and SMN knockdown cells show a Golgi-like pattern of YFP fluorescence. When shifted to the restrictive temperature for 1 hour, SMN depleted cultures had a statistically significant decrease in the number of cells that shifted to an ER-like pattern of fluorescence ($p<0.01$ by Student's t-test). Quantification of 3 separate experiments by a blinded observer shows that by 2hrs, there is no statistically significant difference between control and SMN depleted cultures.

Figure 7: SMN knockdown does not confer sensitivity to thapsigargin

7a) NSC-34 cells were treated with increasing concentrations of Thapsigargin overnight and cell viability was measured using the MTT assay. While knockdown of alpha-COP (4-1-15 DOX) increased the sensitivity to thapsigargin ($p<0.05$), knockdown of SMN (4-56 DOX) had no impact on the toxicity of thapsigargin. These data represent the combined results from three separate experiments.

References

Ayala, I., Colanzi, A., 2017. Alterations of Golgi organization in Alzheimer's disease: A cause or a consequence? Tissue Cell. 49, 133-140.

Bellouze, S., et al., 2014. Golgi fragmentation in pmn mice is due to a defective ARF1/TBCE cross-talk that coordinates COPI vesicle formation and tubulin polymerization. Hum Mol Genet. 23, 5961-75.

Bellouze, S., et al., 2016. Stathmin 1/2-triggered microtubule loss mediates Golgi fragmentation in mutant SOD1 motor neurons. Mol Neurodegener. 11, 43.

Burman, J.L., et al., 2008. Scyl1, mutated in a recessive form of spinocerebellar neurodegeneration, regulates COPI-mediated retrograde traffic. J Biol Chem. 283, 22774-86.

Corrado, L., et al., 2010. Mutations of FUS gene in sporadic amyotrophic lateral sclerosis. J Med Genet. 47, 190-4.

Custer, S.K., et al., 2013. Dilysine motifs in exon 2b of SMN protein mediate binding to the COPI vesicle protein alpha-COP and neurite outgrowth in a cell culture model of spinal muscular atrophy. Hum Mol Genet. 22, 4043-52.

Custer, S.K., Androphy, E.J., 2014. Autophagy dysregulation in cell culture and animals models of spinal muscular atrophy. Mol Cell Neurosci. 61, 133-40.

Dimitriadi, M., et al., 2016. Decreased function of survival motor neuron protein impairs endocytic pathways. Proc Natl Acad Sci U S A. 113, E4377-86.

Farg, M.A., et al., 2013. Ataxin-2 interacts with FUS and intermediate-length polyglutamine expansions enhance FUS-related pathology in amyotrophic lateral sclerosis. Hum Mol Genet. 22, 717-28.

Fifita, J.A., et al., 2017. A novel amyotrophic lateral sclerosis mutation in OPTN induces ER stress and Golgi fragmentation in vitro. Amyotroph Lateral Scler Frontotemporal Degener. 18, 126-133.

Fujita, Y., et al., 2006. Fragmentation of Golgi apparatus of nigral neurons with alpha-synuclein-positive inclusions in patients with Parkinson's disease. Acta Neuropathol. 112, 261-5.

Gabriel, L., Stevens, Z., Melikian, H., 2009. Measuring plasma membrane protein endocytic rates by reversible biotinylation. J Vis Exp.

Gu, F., et al., 1997. Functional dissection of COP-I subunits in the biogenesis of multivesicular endosomes. J Cell Biol. 139, 1183-95.

Haase, G., Rabouille, C., 2015. Golgi Fragmentation in ALS Motor Neurons. New Mechanisms Targeting Microtubules, Tethers, and Transport Vesicles. Front Neurosci. 9, 448.

Han, K.J., et al., 2016. Monoubiquitination of survival motor neuron regulates its cellular localization and Cajal body integrity. Hum Mol Genet. 25, 1392-405.

Hehnly, H., et al., 2010. Cdc42 regulates microtubule-dependent Golgi positioning. Traffic. 11, 1067-78.

Izumi, K., et al., 2016. ARCN1 Mutations Cause a Recognizable Craniofacial Syndrome Due to COPI-Mediated Transport Defects. Am J Hum Genet. 99, 451-9.

Lee, C., Goldberg, J., 2010. Structure of coatomer cage proteins and the relationship among COPI, COPII, and clathrin vesicle coats. Cell. 142, 123-32.

Li, H., et al., 2015. alpha-COP binding to the survival motor neuron protein SMN is required for neuronal process outgrowth. Hum Mol Genet. 24, 7295-307.

Liu, C., et al., 2017. Loss of the golgin GM130 causes Golgi disruption, Purkinje neuron loss, and ataxia in mice. Proc Natl Acad Sci U S A. 114, 346-351.

Luna, A., et al., 2002. Regulation of protein transport from the Golgi complex to the endoplasmic reticulum by CDC42 and N-WASP. Mol Biol Cell. 13, 866-79.

Mali, Y., Zisapel, N., 2010. VEGF up-regulation by G93A superoxide dismutase and the role of malate-aspartate shuttle inhibition. Neurobiol Dis. 37, 673-81.

Nakagomi, S., et al., 2008. A Golgi fragmentation pathway in neurodegeneration. Neurobiol Dis. 29, 221-31.

Ng, S.Y., et al., 2015. Genome-wide RNA-Seq of Human Motor Neurons Implicates Selective ER Stress Activation in Spinal Muscular Atrophy. Cell Stem Cell. 17, 569-84.

Palmisano, R., et al., 2011. Endosomal accumulation of APP in wobbler motor neurons reflects impaired vesicle trafficking: implications for human motor neuron disease. BMC Neurosci. 12, 24.

Pelletier, S., et al., 2012. An early onset progressive motor neuron disorder in Scyl1-deficient mice is associated with mislocalization of TDP-43. J Neurosci. 32, 16560-73.

Peter, C.J., et al., 2011. The COPI vesicle complex binds and moves with survival motor neuron within axons. Hum Mol Genet. 20, 1701-11.

Raykhel, I., et al., 2007. A molecular specificity code for the three mammalian KDEL receptors. J Cell Biol. 179, 1193-204.

Razi, M., Chan, E.Y., Tooze, S.A., 2009. Early endosomes and endosomal coatomer are required for autophagy. J Cell Biol. 185, 305-21.

Ren, Z., et al., 2003. Multiple trafficking signals regulate kainate receptor KA2 subunit surface expression. J Neurosci. 23, 6608-16.

Riessland, M., et al., 2017. Neurocalcin Delta Suppression Protects against Spinal Muscular Atrophy in Humans and across Species by Restoring Impaired Endocytosis. Am J Hum Genet. 100, 297-315.

Schmidt, W.M., et al., 2007. Mutation in the Scyl1 gene encoding amino-terminal kinase-like protein causes a recessive form of spinocerebellar neurodegeneration. EMBO Rep. 8, 691-7.

Selivanova, A., et al., 2006. COPI-mediated retrograde transport is required for efficient gamma-secretase cleavage of the amyloid precursor protein. Biochem Biophys Res Commun. 350, 220-6.

Soo, K.Y., et al., 2015. Rab1-dependent ER-Golgi transport dysfunction is a common pathogenic mechanism in SOD1, TDP-43 and FUS-associated ALS. Acta Neuropathol. 130, 679-97.

Spang, A., Schekman, R., 1998. Reconstitution of retrograde transport from the Golgi to the ER in vitro. J Cell Biol. 143, 589-99.

Szul, T., Sztul, E., 2011. COPII and COPI traffic at the ER-Golgi interface. Physiology (Bethesda). 26, 348-64.

Tarlarini, C., et al., 2015. Novel FUS mutations identified through molecular screening in a large cohort of familial and sporadic amyotrophic lateral sclerosis. Eur J Neurol. 22, 1474-81.

Thyberg, J., Moskalewski, S., 1985. Microtubules and the organization of the Golgi complex. Exp Cell Res. 159, 1-16.

Ting, C.H., et al., 2012. The spinal muscular atrophy disease protein SMN is linked to the Golgi network. PLoS One. 7, e51826.

Todd, A.G., et al., 2013. COPI transport complexes bind to specific RNAs in neuronal cells. Hum Mol Genet. 22, 729-36.

van Dis, V., et al., 2014. Golgi fragmentation precedes neuromuscular denervation and is associated with endosome abnormalities in SOD1-ALS mouse motor neurons. Acta Neuropathol Commun. 2, 38.

Vivithanaporn, P., Yan, S., Swanson, G.T., 2006. Intracellular trafficking of KA2 kainate receptors mediated by interactions with coatomer protein complex I (COPI) and 14-3-3 chaperone systems. J Biol Chem. 281, 15475-84.

Wang, Z.B., Zhang, X., Li, X.J., 2013. Recapitulation of spinal motor neuron-specific disease phenotypes in a human cell model of spinal muscular atrophy. Cell Res. 23, 378-93.

Watkin, L.B., et al., 2015. COPA mutations impair ER-Golgi transport and cause hereditary autoimmune-mediated lung disease and arthritis. Nat Genet. 47, 654-60.

Wen, H.L., et al., 2010. Stathmin, a microtubule-destabilizing protein, is dysregulated in spinal muscular atrophy. Hum Mol Genet. 19, 1766-78.

Xu, X., et al., 2010. Mutation in archain 1, a subunit of COPI coatomer complex, causes diluted coat color and Purkinje cell degeneration. PLoS Genet. 6, e1000956.

Yang, J.S., et al., 2008. A role for phosphatidic acid in COPI vesicle fission yields insights into Golgi maintenance. Nat Cell Biol. 10, 1146-53.

Zhao, Y.O., et al., 2010. Localisation and mislocalisation of the interferon-inducible immunity-related GTPase, Irgm1 (LRG-47) in mouse cells. PLoS One. 5, e8648.

Highlights:

- SMA fibroblasts have abnormal Golgi apparatus morphology which can be rescued by restoring SMN protein levels to normal
- Knockdown of the SMN binding partner α-COP produces a similar diffuse Golgi morphology
- α-COP over-expression restores normal Golgi morphology in SMA fibroblasts
- COPI-dependent intracellular trafficking is altered in cells after knockdown of SMN

Figure 1

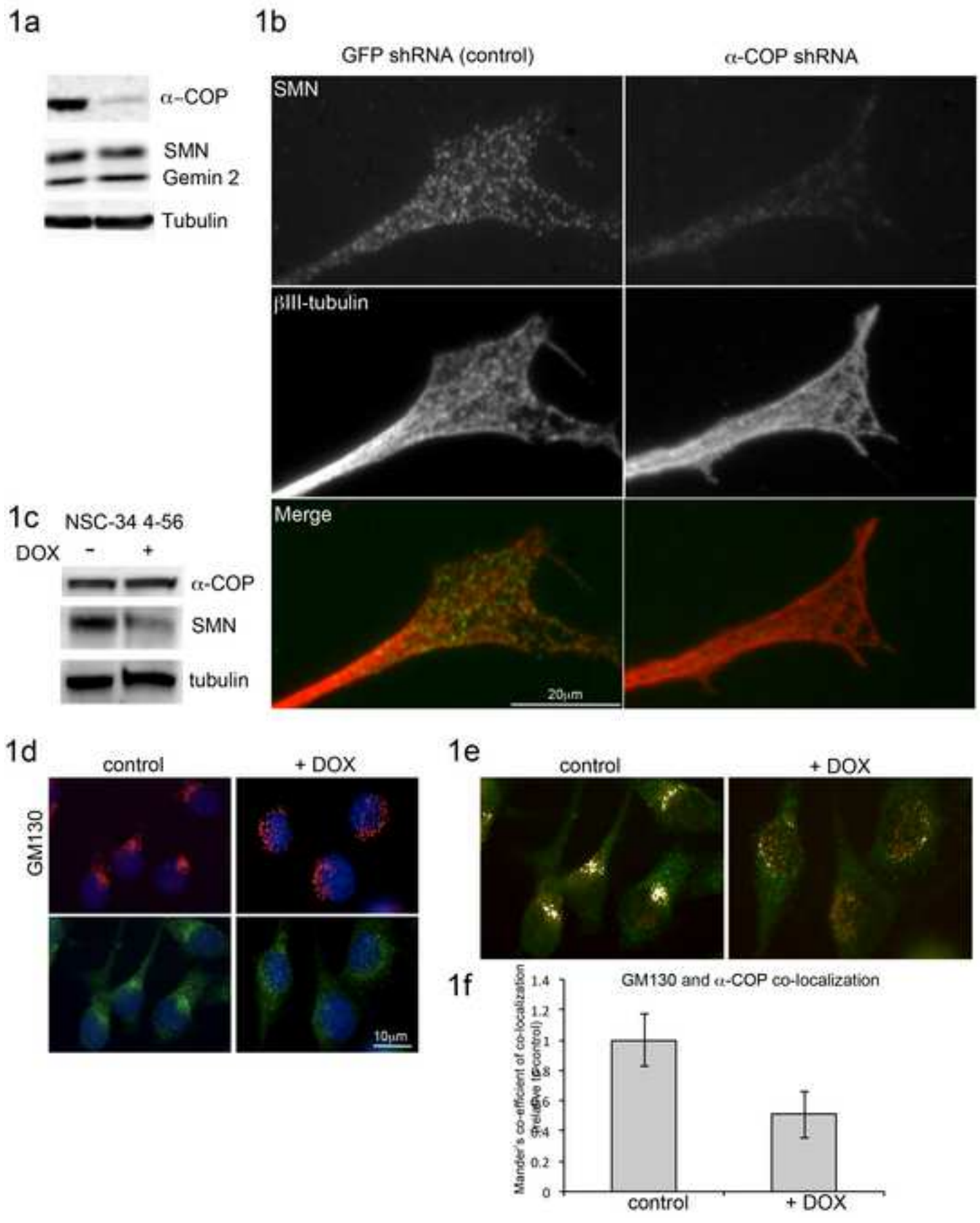

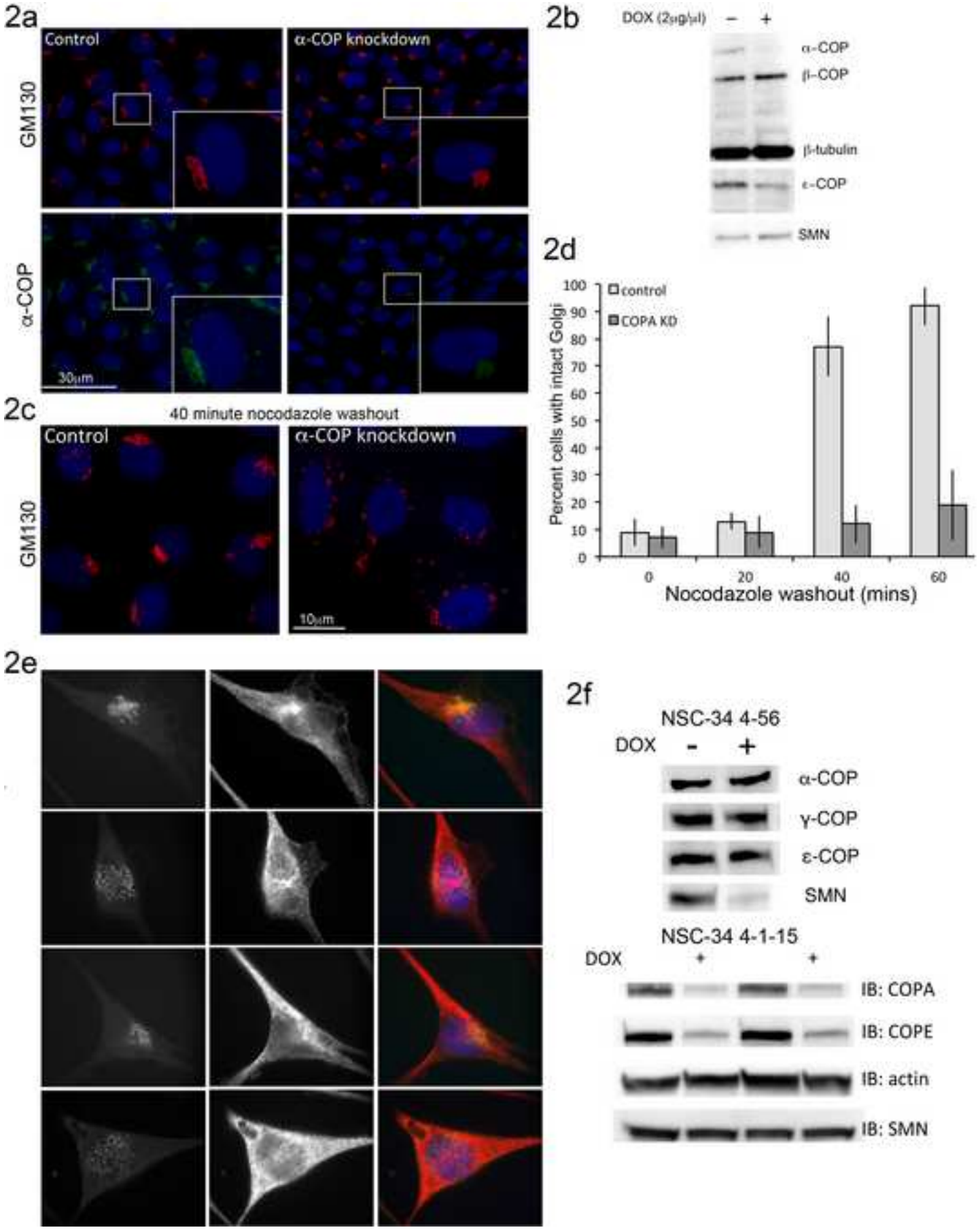

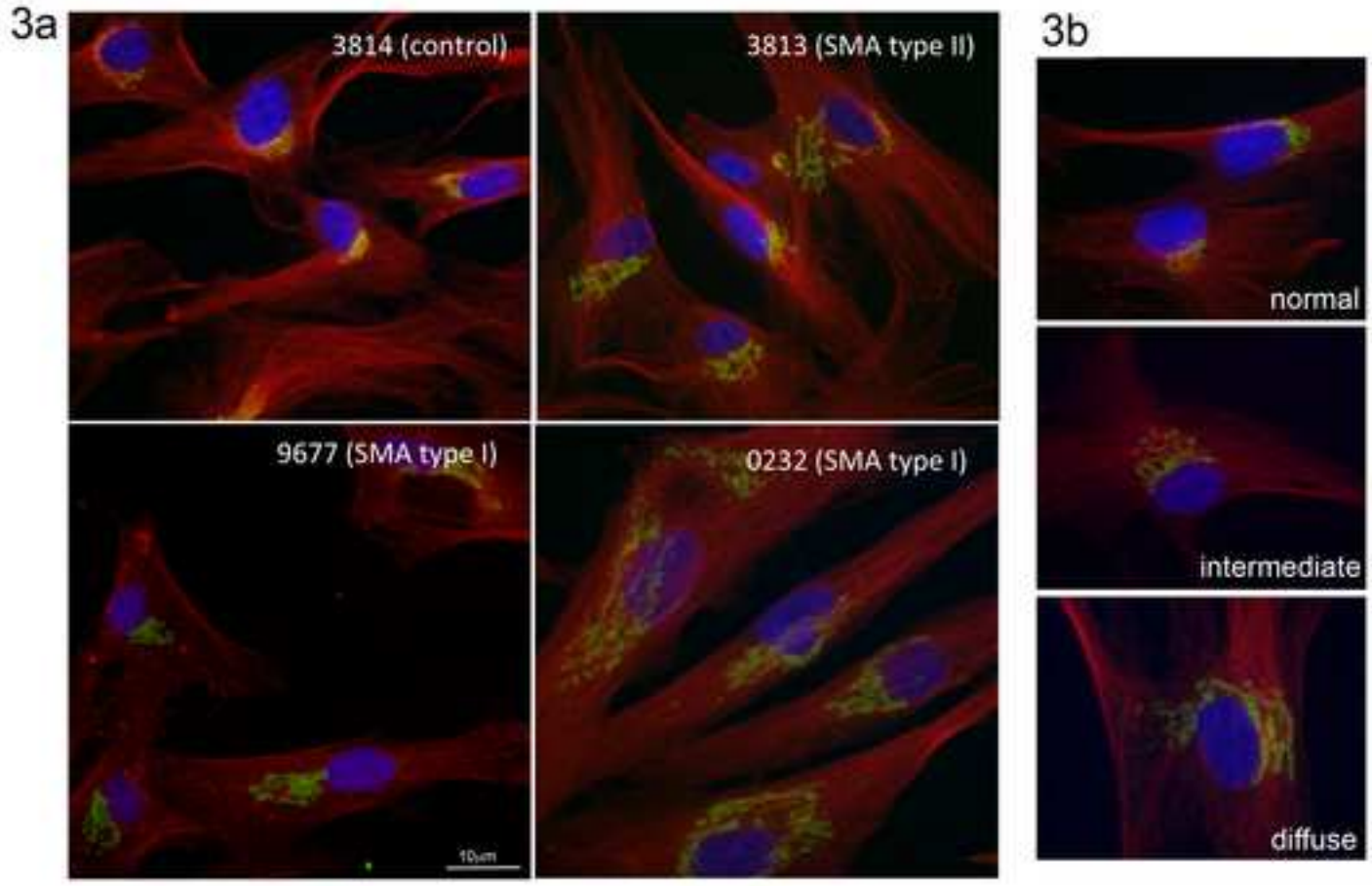

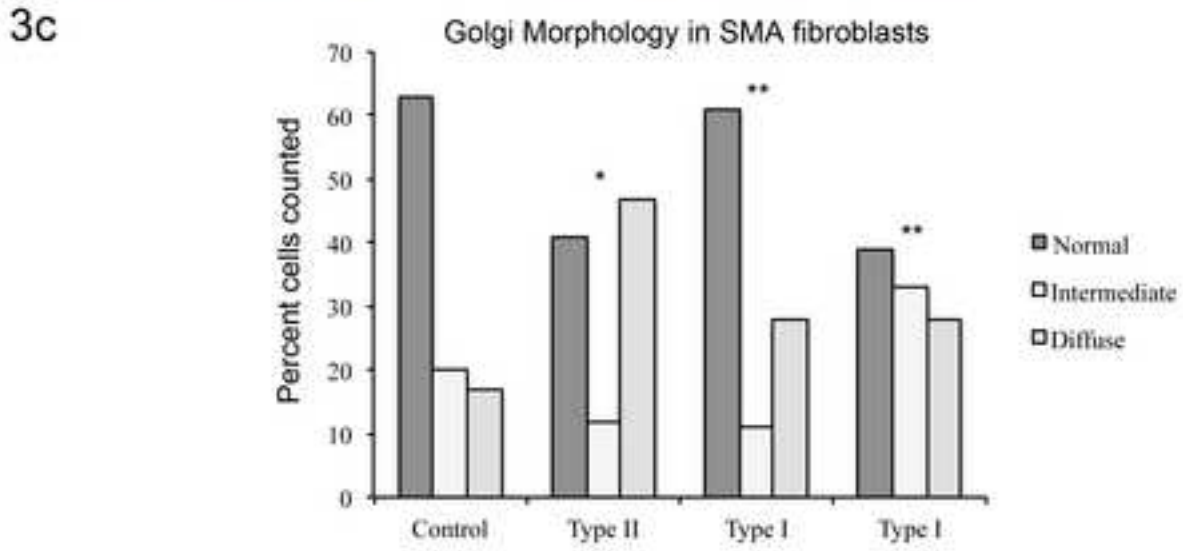

Figure
Click here to download high resolution image

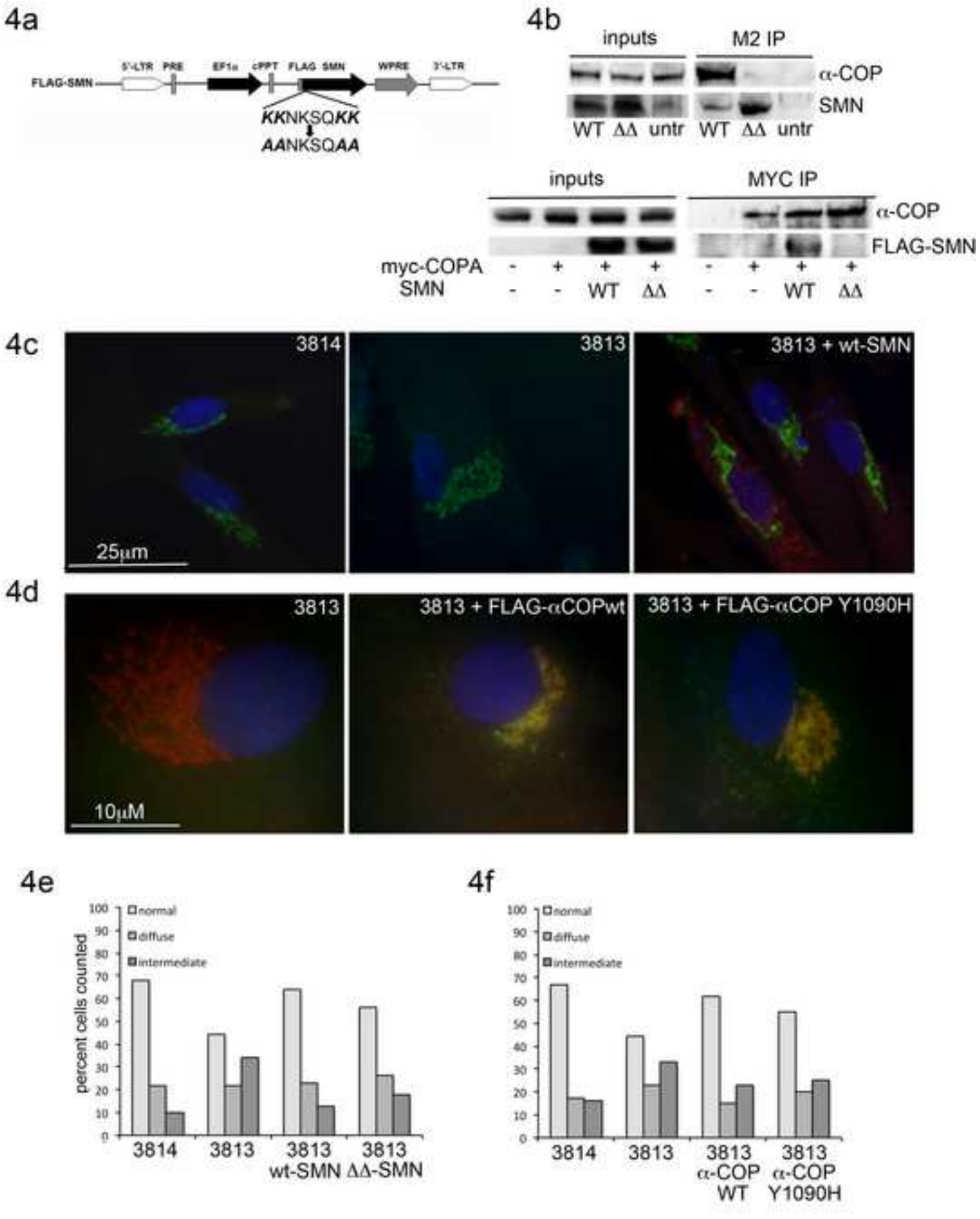

Figure 5

Click here to download high resolution image

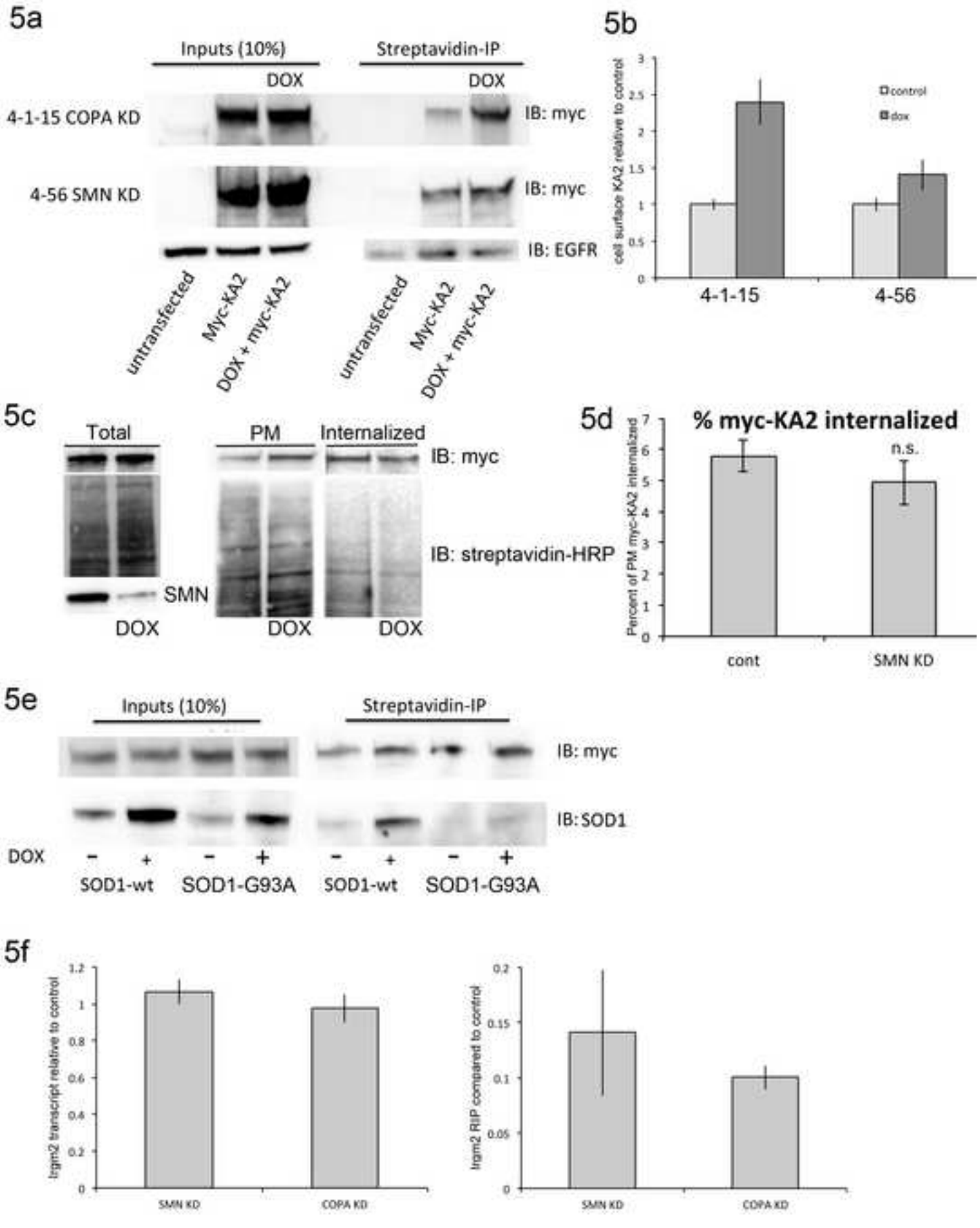

Figure 6

6a

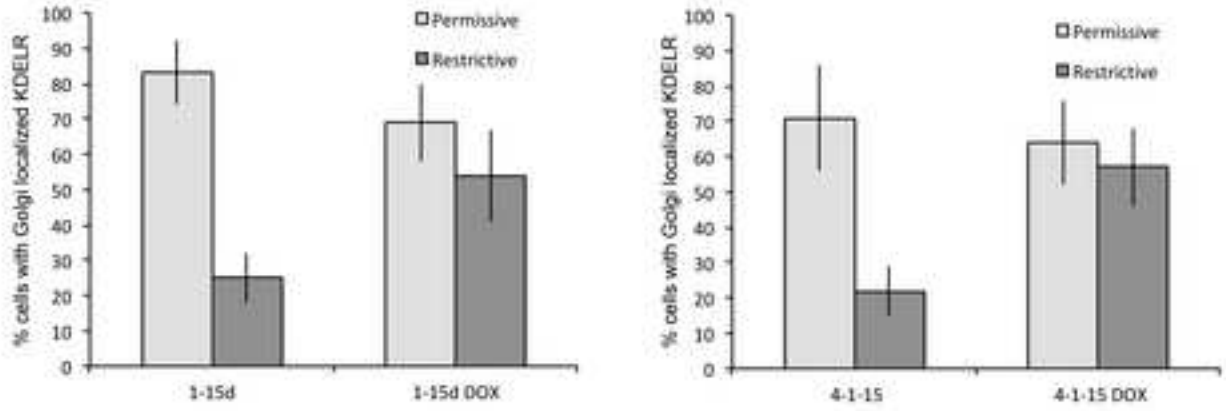

6b

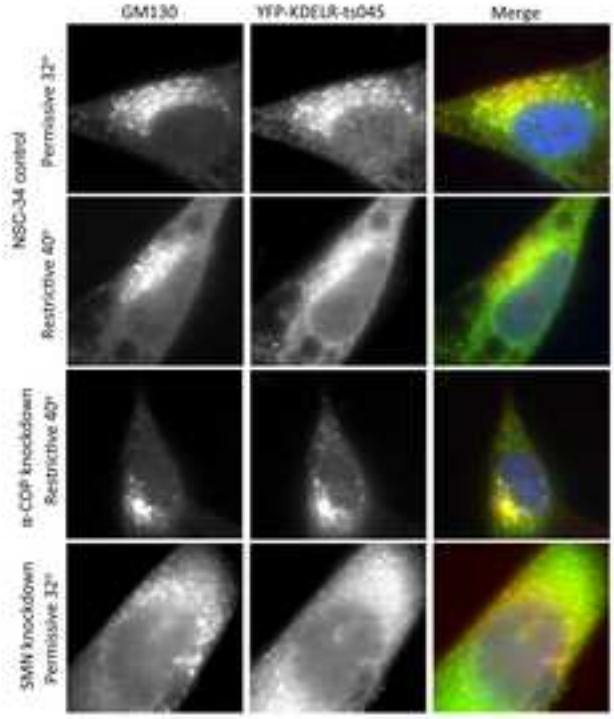

6c

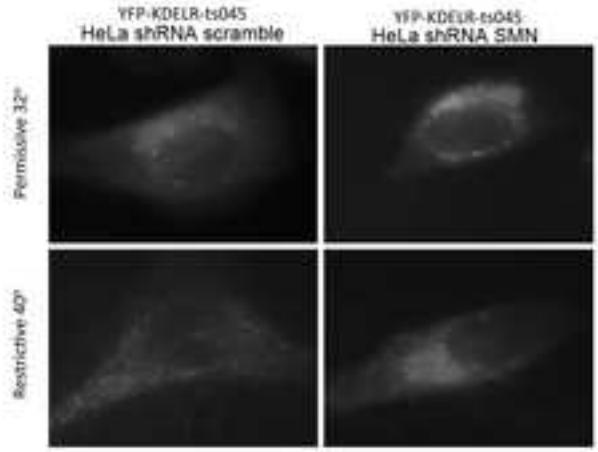

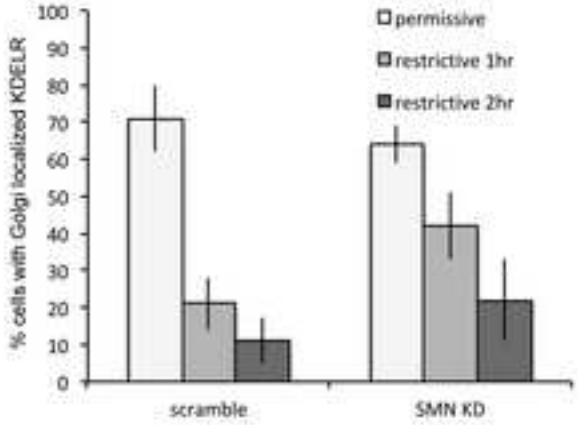

Figure 7

Click here to download high resolution image

7a